Applied Physics A (2022) 128:1083
https://doi.org/10.1007/s00339-022-06210-8

Applied Physics A
Materials Science & Processing

S.I. : 50TH ANNIVERSARY OF APPLIED PHYSICS

Mechanisms for point defect-induced functionality in complex perovskite oxides

Chiara Ricca[1] · **Ulrich Aschauer**[1]

Received: 19 October 2022 / Accepted: 1 November 2022 / Published online: 18 November 2022

Abstract

Perovskite oxides are an extremely versatile class of materials in which functionality can, besides other routes, also be engineered via the deliberate introduction of defects. In this focused review, we will specifically look at mechanistic details of ferroelectric and magnetic functionality introduced, altered, or reinforced by point defects. An ever-growing number of related studies start to provide a basis for the mechanistic understanding of different engineering routes to be exploited in future studies. Nevertheless, this review highlights that the effect of defects is not always easily predicted, given the delicate balance of lattice, charge, spin, and orbital degrees of freedom inherent to the perovskite structure. Systematic studies across various chemistries are thus still very much needed to obtain a more complete basis for defect-engineering ferroelectric and magnetic functionality in perovskite oxides.

Keywords Perovskite oxides · Point defects · Functionality · Mechanisms

Oxides with the ABO_3 perovskite crystal structure (see Fig. 1a) are a chemically extremely diverse class of materials as many elements of the periodic table can be accommodated on the A and B sites [1]. The class of materials is named after the parent compound $CaTiO_3$, other prototypical material examples being $SrTiO_3$, $BaTiO_3$, or $PbTiO_3$. In all perovskites, the B site is octahedrally coordinated with O anions, while the A site is in dodecahedral coordination (see Fig. 1a). The perovskite structure is generally stable when the ionic radii fulfill the criteria of the Goldschmidt tolerance factor

$$t = \frac{r_A + r_O}{\sqrt{2}(r_B + r_O)},$$

which is based on a balance of the anion (r_O) and cation (r_A and r_B) radii to fit both the unit-cell edge (numerator) and diagonal (denominator) [2]. Generally, compositions with a smaller t (i.e., a small A site compared to the B site) will be prone to undergo antiferrodistortive octahedral rotations (see Fig. 1b), while in those with t near unity, the B site may move away from the center of the coordination octahedron (see Fig. 1c). B-site off-centering may additionally also be induced by the chemistry, for example in $PbTiO_3$ due to the presence of lone pairs on the A site [3].

This off-center distortion is of technological relevance as the relative displacement of anions and cations induces a local electrical dipole. If coupled parallel with neighboring dipoles, this leads to polar materials than can be ferroelectric if the dipole direction is switchable by an applied electric field [4, 5]. An antiparallel coupling, at least between some neighboring dipoles, on the other hand, will lead to antiferroelectricity [6]. Ferroelectricity and antiferroelectricity are two functional properties of great relevance. While a ferroelectric can be locally poled to store digital information as a function of the polarization direction (FE-RAM) [4], antiferroelectrics are highly relevant for energy storage [7].

Perovskite oxides may also present magnetic properties, most commonly when the B site has a partially filled d-electron shell. A-site magnetism usually derives from rare-earth elements and, due to the weaker exchange interactions, is limited to very low temperatures. Depending on the exchange interaction between the magnetic sites, the material may assume antiferromagnetic, ferromagnetic, or ferrimagnetic spin configurations [8–10]. Apart from (anti) ferroelectricity and magnetism, perovskite oxides may also

✉ Ulrich Aschauer
ulrich.aschauer@unibe.ch

[1] Department of Chemistry, Biochemistry and Pharmaceutical Sciences, University of Bern, Bern, Switzerland

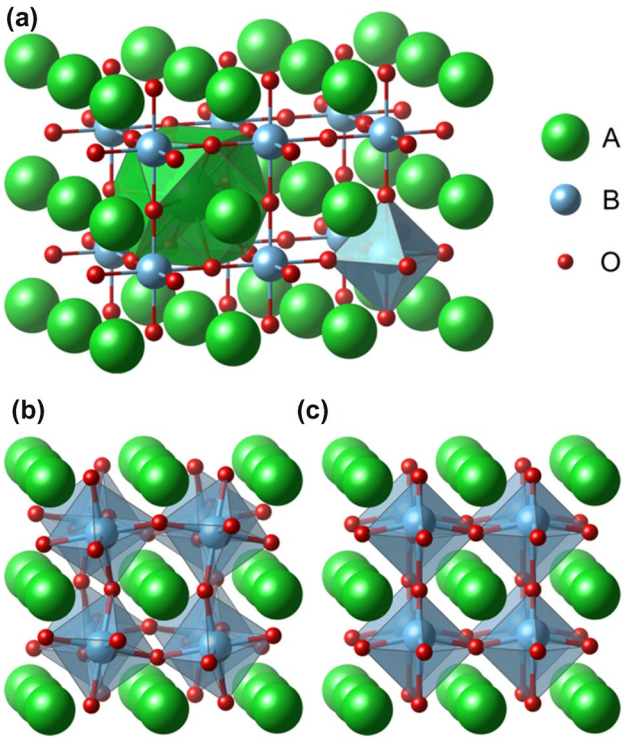

Fig. 1 **a** Perovskite oxide structure, highlighting the octahedrally coordinated B-site and the A-site in dodecahedral coordination, **b** perovskite structure with octahedral rotations and **c** perovskite structure with B-site off-centering

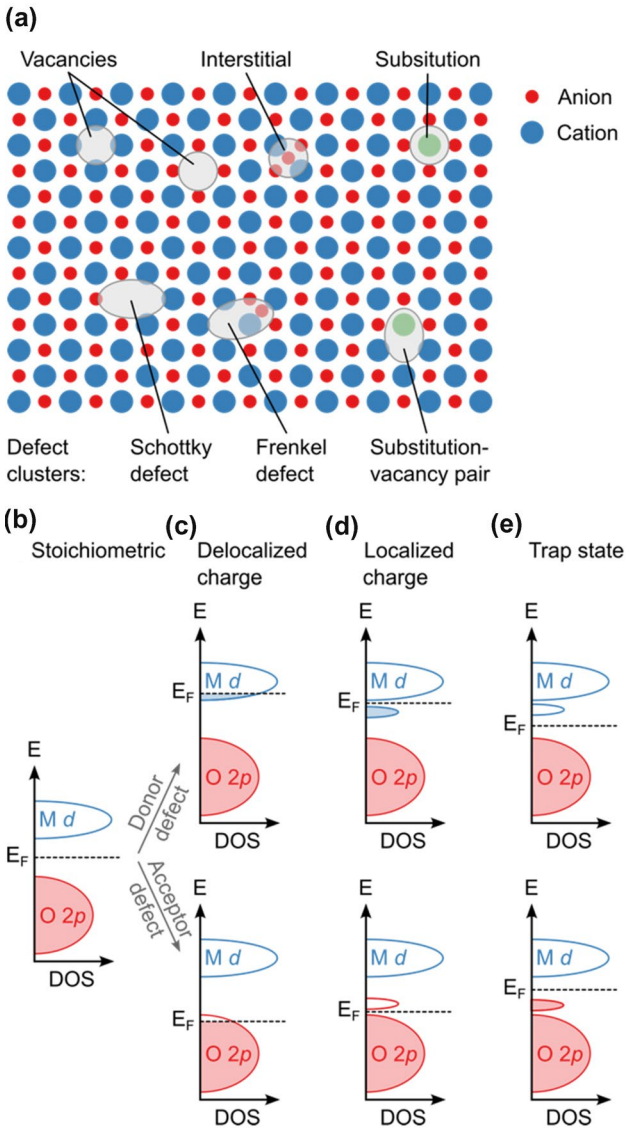

Fig. 2 **a** Types of point defects: anion and cation vacancies, interstitial (anion), substitution (cation) as well as point defects clusters (depicted are Schottky and Frenkel pairs as well as a substitution-anion vacancy pair). Electronic structure changes compared to **b** the stoichiometric structure for donor and acceptor defects when **c** the charge is delocalized, **d** localized, or **e** traps states exist

exhibit functional properties such as superconductivity [11], magnetoresistance [12], or (photo)catalytic activity [13], which we will, however, not focus on here.

Looking at the enormous compositional flexibility, it is surprising how few materials exhibit the above-mentioned functional properties. These properties also do not often coexist [14], magnetoelectric multiferroicity (e.g., coexisting ferroelectricity and magnetism) naturally occurring at room temperature for just a few compositions such as the well-studied $BiFeO_3$ [15].

Engineering perovskite oxides to induce or reinforce functional properties has therefore been an active field of research. The most established engineering approach is coherent epitaxial thin-film growth during which the perovskite material is strained to adopt the lattice parameters of the substrate [16]. This deformation changes the unit-cell geometry, symmetry, and interatomic interactions and may lead to emerging ferroelectricity in nominally non-polar materials [17]. Another approach to engineering properties is by alloying on either of the two cation sites. As such, adding Ba to $SrTiO_3$ is known to promote ferroelectricity [18]. Magnetic properties may also be engineered in this way by aliovalent substitution. The $LaMnO_3$–$SrMnO_3$ solid solution is a prominent example where the two end members are antiferromagnets, while changes in the Mn oxidation state due to the aliovalent A site substitution result in ferromagnetism for intermediate compositions [19].

Another, less-explored route to engineer functional properties is by deliberately inducing point defects or point-defect clusters. Point defects can be missing atoms (vacancies), additional atoms (interstitials), or replaced atoms (substitutions), while clusters refer to aggregates of these individual defects (see Fig. 2a). The stability (i.e., formation energy) and therefore the relative abundance of each type of defect depends on the environment (i.e., elemental chemical

potentials) [20–22]. While point defects are referred to as zero-dimensional (0D) defects, defects may also occur in higher dimensions such as 1D line defects (e.g., dislocations) or 2D planar defects (e.g., grain boundaries, surfaces, or interfaces), which we will, however, not focus on here.

A defect in an ionic or mixed covalent-ionic material will lead to electron excess or deficiency when neutral atoms are removed. In the most typical situation, this leads to delocalized free electrons or holes in the conduction and valence band, respectively (see Fig. 2b). In addition, as the bonding around a defect is altered, states will shift to different energies. In a semiconductor or insulator, these states may appear in the band gap and become preferential sites for excess charge localization (see Fig. 2c). These localized occupied defect states, when located close to either the conduction or valence band edge are referred to as shallow donor and shallow acceptor states, respectively, as thermal excitation from these states to the conduction or valence band, respectively, leads to free carriers. Depending on the crystal chemistry, these states can also be unoccupied or can become unoccupied as a defect assumes a different charge state by electron exchange with a reservoir [20–22]. In such situations, the state can accommodate free electrons or holes and is referred to as a trap state (see Fig. 2d).

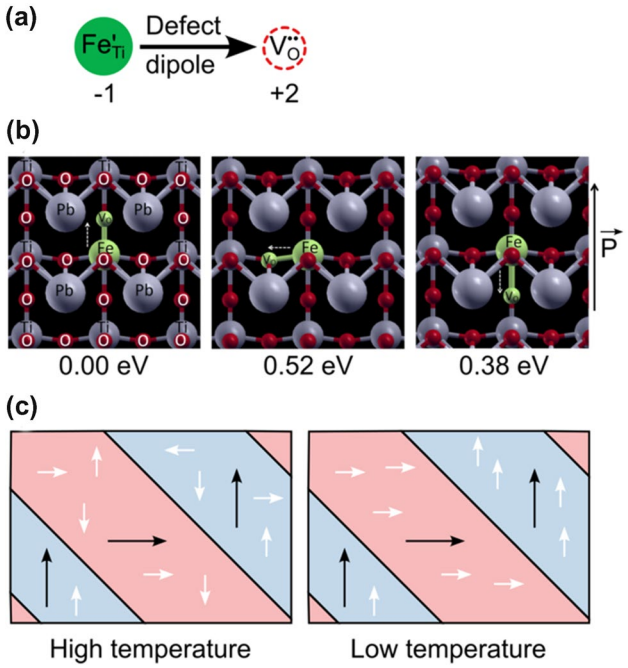

Fig. 3 **a** Schematic of a defect-pair dipole formed between a substitutional Fe atom on a Ti site with a relative charge of − 1 and an oxygen vacancy with a relative charge of + 2 in $PbTiO_3$, **b** Energetics of different alignments of the defect dipole (dashed white arrow) with the lattice polarization $\vec{P}$ reprinted with permission from Ref. [30], Copyright 2013 by the American Physical Society, **c** Schematic 90° domain structure (black arrows) in which defect dipoles (white arrows) align at low temperatures

1 Ferroelectricity induced by defects

1.1 Defect pairs

Defects in ferroelectrics were long considered to be avoided as they are related to degradation phenomena such as leakage, fatigue, and aging [23–28]. More recently, it was recognized that the defect chemistry can be used to tune ferroelectric properties. Most studies considered defect pairs such as $\left[Fe'_{Ti}V^{\cdot\cdot}_{O}\right]^{\cdot}$ in perovskite titanates, using Kröger-Vink notation [29]. These defect pairs involving cation substitution and oxygen vacancies are known to bind, whereas those involving cation substitution and cation vacancies (e.g., $\left[Nb^{\cdot}_{Ti}V''_{Pb}\right]'$ will dissociate [30]. These defect pairs carry a defect dipole between the positively and the negatively charged defect entity (see Fig. 3a) that preferentially aligns with the ferroelectric polarization as shown for the example of a $\left[Fe'_{Ti}V^{\cdot\cdot}_{O}\right]^{\cdot}$ in $PbTiO_3$ in Fig. 3b. Due to their dipolar field, two interacting dipoles will align parallel, when axially aligned but antiparallel when laterally aligned. In a ferroelectric, the axial dipole–dipole interactions dominate over the lateral one, favoring an overall parallel dipole alignment. A defect dipole embedded in such a dipole lattice will also most favorably be aligned parallel with the ferroelectric dipoles. As such it was demonstrated that defects pairs reorient to align with the ferroelectric polarization direction in materials such as $PbTiO_3$ [30–32], $BaTiO_3$ [33], $KNbO_3$ [33], and $BiFeO_3$ [27] upon cooling as schematically shown in Fig. 3c. The defect–dipole reorientation must involve migration, usually of substitutional cation defects or oxygen vacancies. The latter was shown to be energetically significantly more facile (sub-eV migration energies) than cation migration (multi-eV barriers) [34–37]. It should nevertheless be noted that, in defect clusters, the presence of oxygen vacancies can significantly affect migration pathways due to A-site-oxygen bonding optimization leading to a reduction in cation migration energies [34].

Once formed, a state with ordered defect dipoles can pin a certain ferroelectric polarization direction. This effect may require fairly high defect concentrations, as in perovskite manganites the polarizing effect of both $\left[V''_{Sr}V^{\cdot\cdot}_{O}\right]^{x}$ and $\left[Fe'_{Mn}V^{\cdot\cdot}_{O}\right]^{X}$ dipoles was shown to be limited to within a radius of around 6 Å around the defect [37, 38]. Nevertheless, multiscale simulations revealed a longer-range effect [39], which could be due to periodic boundary condition effects in density functional theory or due to the different chemistry (manganite vs. titanate). Since many defect pairs not only carry an electrical dipole but also an elastic dipole, the ordering of the dipoles with external strain, applied for example via heteroepitaxial growth on a substrate with a

different lattice parameter, can be used to impose a preferred defect–dipole orientation via electromechanical coupling [39]. This effect can increase the ferroelectric critical temperature, for example in $BaTiO_3$ from the stoichiometric value of 123 °C [40] up to 800 °C [41].

1.2 Defect clusters

Not only defect pairs but also clusters of more than two defects may result in an electric dipole. As such, it was shown, based on a comparison of density functional theory calculations and spectroscopic experiments, that in $SrTiO_3$ the occurrence of a $V_{Sr} - V_O - V_O$ trivacancy cluster is associated with the emergence of ferroelectricity [42]. In this case, many different relative arrangements of the various individual defects are possible, each having a different net polarization direction.

1.3 Single defects

While defect pairs and defect clusters require a high level of control of the synthesis conditions to form, super- or sub-stoichiometry of a single element, leading to the formation of point defects associated with that element, promise to be easier to control. Indeed, also single point defects can promote ferroelectric properties. As such, cation antisite defects (substitution of Ti on the Sr site or Sr on the Ti site) lead to polar displacements in $SrTiO_3$, Ti_{Sr} more strongly so [36, 43, 44]. The mechanism behind the emerging polarization is a bonding optimization of the cation occupying a too-large site, resulting in off-centering within the coordination polyhedron (see Fig. 4). In this case, clustering of the antisites with oxygen vacancies should be avoided as a reduction in polarization and an increase in switching barrier result [36]. A similar effect was reported in the A-site double perovskite $EuBaTi_2O_6$, where oxygen vacancies lead to a Ti off-centering, in addition to ferromagnetic Eu^{2+}–Ti^{3+}–Eu^{2+} exchange, resulting in a ferroelectric–ferromagnetic multiferroic material [45].

Perovskite oxides with a Jahn–Teller distortion were also shown to lead to polar structures around defects. Stoichiometric $LaMnO_3$ exhibits a cooperative Jahn–Teller distortion with alternating long and short Mn–O bonds within a {001} plane [46, 47]. Relaxations around an oxygen vacancy alter these bond lengths and therefore orbital energies, leading to an asymmetric accommodation of the excess electrons at Mn in next-nearest neighbor positions to the defect, resulting in a net polarization around the defect [48].

The cation order in perovskite oxide superlattices offers an additional degree of freedom in obtaining a net polarization due to oxygen vacancies. It was shown that a stoichiometric $(LaFeO_3)_2/(SrFeO_3)$ superlattice (i.e., a ferrite perovskite with a LaO–LaO–SrO A-site layer sequence) adopts an

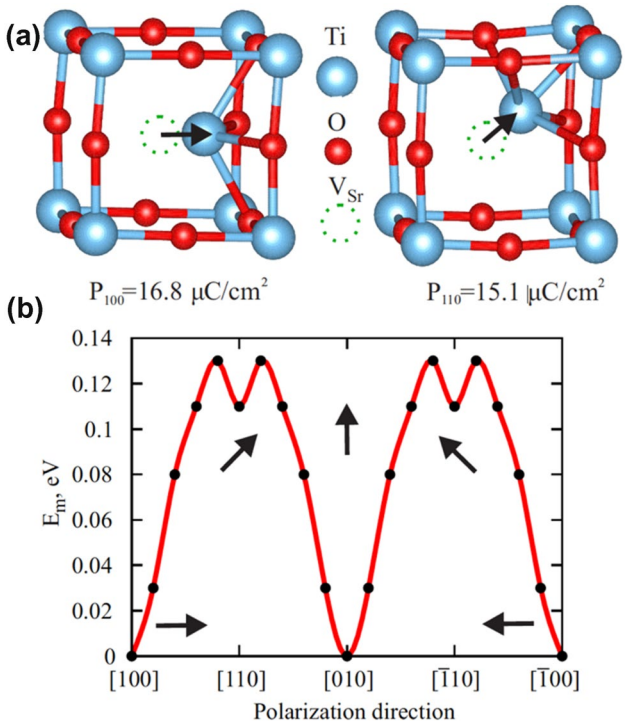

Fig. 4 **a** Ti_{Sr} antisite defect off-centered along [001] and [110] as well as **b** the energy profile associated with migration between these positions, showing that the [100] direction is most favorable. Reprinted figure with permission from Ref. [36] Copyright 2017 by the American Physical Society

antipolar Fe displacement [49]. This antipolar pattern results from hole localization in the FeO_2 layer surrounded by two LaO layers (i.e., the formal Fe oxidation state in these layers is Fe^{4+} whereas the other Fe ions are Fe^{3+}). This hole localization also favors oxygen vacancy formation in the FeO_2 layer between two LaO layers, as the two excess electrons most favorably reduce the Fe^{4+} ions to Fe^{3+}. This reduction, in turn, counteracts the antipolar displacement and favors a polar one in the presence of oxygen vacancies [49].

Just like defect-pair dipoles can be controlled by epitaxial strain [41], also single defects may have anisotropic elastic dipoles [50] than can interact with a strain field leading for example to oxygen vacancy ordering [51]. Such ordering is crucial as only a structure with ordered oxygen vacancies can lead to long-range polar and ferroelectric properties.

2 Magnetism induced or altered by defects

Defect-induced or controlled magnetism is a rich and established field of research, a full review of which would go beyond the goals of the present article, and we will here focus on examples that highlight the mechanisms by which magnetism can be affected by defects.

Both oxygen and Ti deficiency were predicted to result in ferromagnetism in nominally nonmagnetic $SrTiO_3$ [52], a result later confirmed by experiment in $BaTiO_3$ [53]. We want to note, however, the extreme sensitivity of both experimental synthesis and theoretical methods in obtaining non-magnetic or magnetic phases [54, 55]. The mechanism underlying this emergence of magnetism in presence of oxygen vacancies is unpaired excess electrons on the reduced Ti^{3+} sites. Since the concentration of magnetic Ti^{3+} sites is linked with the oxygen vacancy concentration, highly deficient materials are required for long-range magnetic order.

The above examples referred to cases where nominally d^0 Ti^{4+} ions were reduced to potentially magnetic Ti^{3+} ions. Oxygen vacancies may, however, also lead to the emergence of magnetism for non-d^0 ions. One such case is $LaCoO_3$, which is normally non-magnetic due to a full occupation of the t_{2g} states in the low-spin d^6 configuration in an octahedral crystal field. Oxygen vacancies lead to both reduction of Co^{3+} to Co^{2+} and a transition to a high-spin state (see Fig. 5) [56]. The unpaired electrons in Co^{2+} result in a ferromagnetic state in oxygen-deficient $LaCoO_3$. Epitaxial strain was shown to affect the ordering and concentration of oxygen vacancies and hence the Co^{2+} ions, modulating the stability of the long-range ferromagnetic order [57]. A defect-free strain accommodation mechanism with modulation of lattice spacing and hence crystal field was, however, reported to result in a similar stabilization of the ferromagnetic order [58].

Oxygen vacancies can also be used to alter an existing magnetic order. In $EuTiO_3$, the creation of Eu and O vacancy pairs alters the geometry and results in a weakening of the antiferromagnetic Eu–Ti–Eu interactions while introducing ferromagnetic Eu–O–Eu exchange, leading to a transition from antiferromagnetism to ferromagnetism [59]. Spin-polarized Ti^{3+} sites were invoked for an antiferromagnetic to ferromagnetic transition in oxygen-deficient $EuBaTi_2O_6$, where the antiferromagnetic Eu^{2+}–Eu^{2+} exchange in the stoichiometric material is dominated by ferromagnetic Eu^{2+}–Ti^{3+}–Eu^{2+} exchange in presence of oxygen vacancies [60]. Epitaxial strain in conjunction with oxygen vacancies can lead to further changes in the magnetic order. For example, multiferroic $BiCoO_3$ assumes a supertetragonal phase in which Co is in square-pyramidal coordination [61]. The Co sites adopt a *C* type antiferromagnetic order in the bulk, which is retained in presence of oxygen vacancies. However, while tensile epitaxial strain in stoichiometric $BiCoO_3$ results in a transition to G-type antiferromagnetic order, it yields a ferrimagnetic state in the oxygen-deficient structure due to the reduction of Co magnetic moments around the defect. Similar results were reported for antiferromagnetic $LaMnO_3$ thin films, where oxygen deficiency leads to mixed Mn^{3+} and Mn^{4+} oxidation states, that couple ferromagnetically [62].

The alteration of exchange becomes richer in double perovskites with two different magnetic B sites, as the cation order and oxidation states of both B sites may change. La_2CoMnO_6 with a checkerboard B-site order is ferromagnetic due to the dominant exchange interaction between Co^{2+} and Mn^{4+} ions. Reduction via oxygen vacancy formation preferentially occurs on the Mn sites, while oxidation via Sr doping on the A-site affects the Co sites [63]. In both cases, the Curie temperature is lowered as the vacancy and Sr defects induce strong antiferromagnetic exchange or reduce the strength of ferromagnetic exchange, respectively. In La_2NiMnO_6, the presence of excess electrons, for example, due to oxygen vacancy formation or a polar catastrophe mechanism, can alter the checkerboard to a columnar order, introducing antiferromagnetic Mn–Mn and Ni–Ni superexchange in addition to the ferromagnetic Mn–Ni interactions [64]. In agreement with this result, extended oxygen anneal resulted in a reduced oxygen vacancy concentration and lead to stronger ferromagnetism in this material [65].

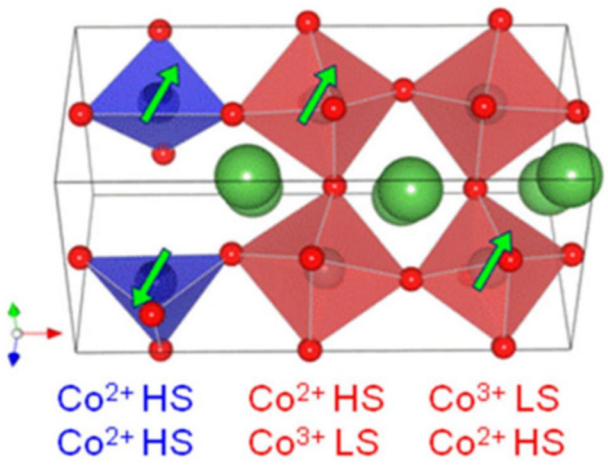

Fig. 5 Oxygen-deficient $LaCoO_3$ with polyhedra adjacent to the defect shown in blue. Arrows show the magnetic moments arising on reduced high-spin Co^{2+}, while low-spin Co^{3+} remain non-magnetic. Reprinted figure with permission from Ref. [56] Copyright (2014) by the American Physical Society

3 Conclusions and outlook

As the above examples have shown, defects can be a rich source of added or altered functionality in perovskite oxides. Defect dipoles resulting from defect pairs or defect clusters couple with the ferroelectric polarization and can locally promote a certain polarization direction. In some cases, single defects can also lead to local polarization effects. In both situations, the fact that electric defect dipoles usually go along with elastic dipoles allows their manipulation with epitaxial strain. The resulting ordered electric defect dipoles

strongly promote a polar state and dramatically increase the ferroelectric Curie temperature.

On the other hand, defects lead to changes in oxidation state and exchange pathways that can induce magnetism in otherwise non-magnetic materials or alter an existing magnetic order, for example from antiferromagnetic to ferromagnetic.

Defects thus hold great promise to engineer both properties in perovskite oxides, in particular inducing ferroelectricity in already (anti)ferromagnetic materials or magnetism in ferroelectric materials to obtain magnetoelectric multiferroics. Despite this promise, a rational design of these properties is still hampered by the lack of a general understanding and predictability of defect-induced functionality. This primarily stems from the fact that defects induce complicated alterations in both the ionic and electronic structures. Since the physics of stoichiometric perovskite oxides is already dominated by an intricate interplay of lattice, charge, spin, and orbital degrees of freedom, the effect of defects is not always easily foreseen. This is further complicated in double perovskites and thin films/superlattices, where order/disorder phenomena and altered electrostatic boundary conditions, respectively, affect charge localization and defect stability. As a result, excess charge localization, which is at the origin of both defect dipoles and changes in magnetism, is not readily predicted without resorting to involved experiments such as scanning transmission microscopy, electron energy loss spectroscopy, or computational investigations at a high level of theory. Nevertheless, it seems hopeful that the ever-growing number of such studies will eventually lead to sufficient data for a mechanistic understanding of defect-induced ferroelectric and magnetic functionality and hence their rational engineering across the wide compositional range offered by perovskite oxides.

Funding Open access funding provided by University of Bern.

Data availability Data sharing is not applicable to this article as no new data were created or analyzed in this study.

References

1. M.A. Peña, J.L.G. Fierro, Chemical structures and performance of perovskite oxides. Chem. Rev. **101**, 1981–2018 (2001). https://doi.org/10.1021/cr980129f
2. V.M. Goldschmidt, Die Gesetze der Krystallochemie. Naturwissenschaften **14**, 477–485 (1926). https://doi.org/10.1007/bf01507527
3. R.E. Cohen, Origin of ferroelectricity in perovskite oxides. Nature **358**, 136–138 (1992). https://doi.org/10.1038/358136a0
4. J.F. Scott, Applications of modern ferroelectrics. Science **315**(954), 959 (2007). https://doi.org/10.1126/science.1129564
5. J.F. Scott, A review of ferroelectric switching. Ferroelectrics **503**, 117–132 (2016). https://doi.org/10.1080/00150193.2016.1236611
6. C. Kittel, Theory of antiferroelectric crystals. Phys Rev. **82**, 729–732 (1951). https://doi.org/10.1103/physrev.82.729
7. Z. Liu, T. Lu, J. Ye, G. Wang, X. Dong, R. Withers, Y. Liu, Antiferroelectrics for energy storage applications: a review. Adv. Mater. Technolo. **3**, 1800111 (2018). https://doi.org/10.1002/admt.201800111
8. J.B. Goodenough, Theory of the role of covalence in the perovskite-type manganites [La, M(II)]MnO_3. Phys. Rev. **100**, 564–573 (1955). https://doi.org/10.1103/physrev.100.564
9. J.B. Goodenough, An interpretation of the magnetic properties of the perovskite-type mixed crystals $La_{1-x}Sr_xCoO_{3-\lambda}$. J. Phys. Chem. Solids. **6**, 287–297 (1958). https://doi.org/10.1016/0022-3697(58)90107-0
10. J. Kanamori, Superexchange interaction and symmetry properties of electron orbitals. J. Phys. Chem. Solids **10**, 87–98 (1959). https://doi.org/10.1016/0022-3697(59)90061-7
11. J.G. Bednorz, K.A. Müller, Perovskite-type oxides-the new approach to high-Tc superconductivity. Rev. Mod. Phys. **60**, 585–600 (1988). https://doi.org/10.1103/revmodphys.60.585
12. Y. Tokura, Y. Tomioka, H. Kuwahara, A. Asamitsu, Y. Moritomo, M. Kasai, Origins of colossal magnetoresistance in perovskite-type manganese oxides (invited). J. Appl. Phys. **79**, 5288 (1996). https://doi.org/10.1063/1.361353
13. J. Hwang, R.R. Rao, L. Giordano, Y. Katayama, Y. Yu, Y. Shao-Horn, Perovskites in catalysis and electrocatalysis. Science **358**, 751–756 (2017). https://doi.org/10.1126/science.aam7092
14. N.A. Hill, Why are there so few magnetic ferroelectrics? J Phys Chem B. **104**, 6694–6709 (2000). https://doi.org/10.1021/jp000114x
15. G. Catalan, J.F. Scott, Physics and applications of bismuth ferrite. Adv. Mater. **21**, 2463–2485 (2009). https://doi.org/10.1002/adma.200802849
16. D.G. Schlom, L.-Q. Chen, C.-B. Eom, K.M. Rabe, S.K. Streiffer, J.-M. Triscone, Strain tuning of ferroelectric thin films. Annu. Rev. Mater. Res. **37**, 589–626 (2007). https://doi.org/10.1146/annurev.matsci.37.061206.113016
17. J.M. Rondinelli, N.A. Spaldin, Structure and properties of functional oxide thin films: insights from electronic-structure calculations. Adv.Mater. **23**, 3363–3381 (2011). https://doi.org/10.1002/adma.201101152
18. V.V. Lemanov, E.P. Smirnova, P.P. Syrnikov, E.A. Tarakanov, Phase transitions and glasslike behavior in $Sr_{1-x}Ba_xTiO_3$. Phys. Rev. B. **54**, 3151–3157 (1996). https://doi.org/10.1103/physrevb.54.3151
19. A. Urushibara, Y. Moritomo, T. Arima, A. Asamitsu, G. Kido, Y. Tokura, Insulator-metal transition and giant magnetoresistance in $La_{1-x}Sr_xMnO_3$. Phys. Rev. B. **51**, 14103–14109 (1995). https://doi.org/10.1103/physrevb.51.14103
20. S.B. Zhang, J.E. Northrup, Chemical potential dependence of defect formation energies in GaAs: application to Ga

self-diffusion. Phys. Rev. Lett. **67**, 2339–2342 (1991). https://doi.org/10.1103/physrevlett.67.2339
21. J.E. Northrup, S.B. Zhang, Dopant and defect energetics: Si in GaAs. Phys. Rev. B. **47**, 6791–6794 (1993). https://doi.org/10.1103/physrevb.47.6791
22. C. Freysoldt, B. Grabowski, T. Hickel, J. Neugebauer, G. Kresse, A. Janotti, C.G.V. de Walle, First-principles calculations for point defects in solids. Rev. Mod. Phys. **86**, 253–305 (2014). https://doi.org/10.1103/revmodphys.86.253
23. U. Robels, G. Arlt, Domain wall clamping in ferroelectrics by orientation of defects. J. Appl. Phys. **73**, 3454–3460 (1993). https://doi.org/10.1063/1.352948
24. W.L. Warren, G.E. Pike, K. Vanheusden, D. Dimos, B.A. Tuttle, J. Robertson, Defect-dipole alignment and tetragonal strain in ferroelectrics. J. Appl. Phys. **79**, 9250 (1996). https://doi.org/10.1063/1.362600
25. X. Ren, Large electric-field-induced strain in ferroelectric crystals by point-defect-mediated reversible domain switching. Nat. Mater. **3**, 91–94 (2004). https://doi.org/10.1038/nmat1051
26. D.C. Lupascu, Y.A. Genenko, N. Balke, Aging in ferroelectrics. J. Am. Ceram. Soc. **89**, 224–229 (2006). https://doi.org/10.1111/j.1551-2916.2005.00663.x
27. C.M. Folkman, S.H. Baek, C.T. Nelson, H.W. Jang, T. Tybell, X.Q. Pan, C.-B. Eom, Study of defect-dipoles in an epitaxial ferroelectric thin film. Appl. Phys. Lett. **96**, 052903 (2010). https://doi.org/10.1063/1.3298362
28. Y.A. Genenko, J. Glaum, M.J. Hoffmann, K. Albe, Mechanisms of aging and fatigue in ferroelectrics. Mater. Sci. Eng. B **192**, 52–82 (2015). https://doi.org/10.1016/j.mseb.2014.10.003
29. F.A. Kröger, H.J. Vink, Relations between the concentrations of imperfections in crystalline solids. Solid State Phys. **3**, 307–435 (1956). https://doi.org/10.1016/s0081-1947(08)60135-6
30. A. Chandrasekaran, D. Damjanovic, N. Setter, N. Marzari, Defect ordering and defect–domain-wall interactions in $PbTiO_3$: A first-principles study. Phys. Rev. B **88**, 214116 (2013). https://doi.org/10.1103/physrevb.88.214116
31. P. Erhart, P. Träskelin, K. Albe, Formation and switching of defect dipoles in acceptor-doped lead titanate: a kinetic model based on first-principles calculations. Phys. Rev. B **88**, 024107 (2013). https://doi.org/10.1103/physrevb.88.024107
32. P. Marton, C. Elsässer, Switching of a substitutional-iron/oxygen-vacancy defect complex in ferroelectric $PbTiO_3$ from first principles. Phys. Rev. B **83**, 020106 (2011). https://doi.org/10.1103/physrevb.83.020106
33. A.V. Kimmel, P.M. Weaver, M.G. Cain, P.V. Sushko, Defect-mediated lattice relaxation and domain stability in ferroelectric oxides. Phys. Rev. Lett **109**, 117601 (2012). https://doi.org/10.1103/physrevlett.109.117601
34. A. Walsh, C.R.A. Catlow, A.G.H. Smith, A.A. Sokol, S.M. Woodley, Strontium migration assisted by oxygen vacancies in $SrTiO_3$ from classical and quantum mechanical simulations. Phys. Rev. B **83**, 220301 (2011). https://doi.org/10.1103/physrevb.83.220301
35. D.D. Cuong, B. Lee, K.M. Choi, H.-S. Ahn, S. Han, J. Lee, Oxygen vacancy clustering and electron localization in oxygen-deficient $SrTiO_3$: LDA+U study. Phys. Rev. Lett. **98**, 115503 (2007). https://doi.org/10.1103/physrevlett.98.115503
36. K. Klyukin, V. Alexandrov, Effect of intrinsic point defects on ferroelectric polarization behavior of $SrTiO_3$. Phys. Rev. B **95**, 035301 (2017). https://doi.org/10.1103/physrevb.95.035301
37. C. Ricca, D. Berkowitz, U. Aschauer, Ferroelectricity promoted by cation/anion divacancies in $SrMnO_3$. J. Mater. Chem. C **9**, 13321–13330 (2021). https://doi.org/10.1039/d1tc02317a
38. C. Ricca, U. Aschauer, Interplay between polarization, strain, and defect pairs in Fe-doped $SrMnO_{3-\delta}$. Phys. Rev. Res. **3**, 033237 (2021). https://doi.org/10.1103/physrevresearch.3.033237
39. S. Liu, R.E. Cohen, Multiscale simulations of defect dipole–enhanced electromechanical coupling at dilute defect concentrations. Appl. Phys. Lett. **111**, 082903 (2017). https://doi.org/10.1063/1.4989670
40. K. Sakayori, Y. Matsui, H. Abe, E. Nakamura, M. Kenmoku, T. Hara, D. Ishikawa, A. Kokubu, K. Hirota, T.I.T. Ikeda, Curie temperature of $BaTiO_3$. Jpn. J. Appl. Phys. **34**, 5443 (1995). https://doi.org/10.1143/jjap.34.5443
41. A.R. Damodaran, E. Breckenfeld, Z. Chen, S. Lee, L.W. Martin, Enhancement of ferroelectric curie temperature in $BaTiO_3$ films via strain-induced defect dipole alignment. Adv. Mater. **26**, 6341–6347 (2014). https://doi.org/10.1002/adma.201400254
42. Y.S. Kim, J. Kim, S.J. Moon, W.S. Choi, Y.J. Chang, J.-G. Yoon, J. Yu, J.-S. Chung, T.W. Noh, Localized electronic states induced by defects and possible origin of ferroelectricity in strontium titanate thin films. Appl. Phys. Lett. **94**, 202906 (2009). https://doi.org/10.1063/1.3139767
43. M. Choi, F. Oba, I. Tanaka, Role of Ti antisitelike defects in $SrTiO_3$. Phys Rev Lett. **103**, 185502 (2009). https://doi.org/10.1103/physrevlett.103.185502
44. F. Yang, Q. Zhang, Z. Yang, J. Gu, Y. Liang, W. Li, W. Wang, K. Jin, L. Gu, J. Guo, Room-temperature ferroelectricity of $SrTiO_3$ films modulated by cation concentration. Appl. Phys. Lett. **107**, 082904 (2015). https://doi.org/10.1063/1.4929610
45. W. Li, Q. He, L. Wang, H. Zeng, J. Bowlan, L. Ling, D.A. Yarotski, W. Zhang, R. Zhao, J. Dai, J. Gu, S. Shen, H. Guo, L. Pi, H. Wang, Y. Wang, I.A. Velasco-Davalos, Y. Wu, Z. Hu, B. Chen, R.-W. Li, Y. Sun, K. Jin, Y. Zhang, H.-T. Chen, S. Ju, A. Ruediger, D. Shi, A.Y. Borisevich, H. Yang, Manipulating multiple order parameters via oxygen vacancies: the case of $Eu_{0.5}Ba_{0.5}TiO_3{-}\delta$. Phys. Rev. B **96**, 115105 (2017). https://doi.org/10.1103/physrevb.96.115105
46. P. Norby, I.G.K. Andersen, E.K. Andersen, N.H. Andersen, The crystal structure of lanthanum manganite (III), $LaMnO_3$, at room temperature and at 1273 K under N_2. J. Solid State Chem. **119**, 191–196 (1995). https://doi.org/10.1016/0022-4596(95)80028-n
47. J. Rodríguez-Carvajal, M. Hennion, F. Moussa, A.H. Moudden, L. Pinsard, A. Revcolevschi, Neutron-diffraction study of the Jahn–Teller transition in stoichiometric $LaMnO_3$. Phys. Rev. B **57**, R3189–R3192 (1998). https://doi.org/10.1103/physrevb.57.r3189
48. C. Ricca, N. Niederhauser, U. Aschauer, Local polarization in oxygen-deficient $LaMnO_3$ induced by charge localization in the Jahn–Teller distorted structure. Phys. Rev. Res. **2**, 042040 (2020). https://doi.org/10.1103/physrevresearch.2.042040
49. R. Mishra, Y.-M. Kim, J. Salafranca, S.K. Kim, S.H. Chang, A. Bhattacharya, D.D. Fong, S.J. Pennycook, S.T. Pantelides, A.Y. Borisevich, Oxygen-vacancy-induced polar behavior in $(LaFeO_3)_2/(SrFeO_3)$ superlattices. Nano. Lett. **14**, 2694–2701 (2014). https://doi.org/10.1021/nl500601d
50. D.A. Freedman, D. Roundy, T.A. Arias, Elastic effects of vacancies in strontium titanate: Short- and long-range strain fields, elastic dipole tensors, and chemical strain. Phys. Rev. B **80**, 064108 (2009). https://doi.org/10.1103/physrevb.80.064108
51. U. Aschauer, R. Pfenninger, S.M. Selbach, T. Grande, N.A. Spaldin, Strain-controlled oxygen vacancy formation and ordering in $CaMnO_3$. Phys. Rev. B **88**, 10423 (2013). https://doi.org/10.1103/physrevb.88.054111
52. I.R. Shein, A.L. Ivanovskii, First principle prediction of vacancy-induced magnetism in non-magnetic perovskite $SrTiO_3$. Phys. Lett. A **371**, 155–159 (2007). https://doi.org/10.1016/j.physleta.2007.06.013
53. F. Yang, K. Jin, H. Lu, M. He, C. Wang, J. Wen, G. Yang, Oxygen vacancy induced magnetism in $BaTiO_{3-\delta}$ and Nb:$BaTiO_{3-\delta}$ thin films. Sci. China Phys. Mech. Astronomy **53**, 852–855 (2010). https://doi.org/10.1007/s11433-010-0187-x

54. C. Ricca, I. Timrov, M. Cococcioni, N. Marzari, U. Aschauer, Self-consistent DFT+U+V study of oxygen vacancies in $SrTiO_3$. Phys. Rev. Res. **2**, 023313 (2020). https://doi.org/10.1103/physrevresearch.2.023313
55. A. Raeliarijaona, H. Fu, Ferromagnetism in ferroelectric $BaTiO_3$ induced by vacancies: Sensitive dependence on charge state, origin of magnetism, and temperature range of existence. Phys. Rev. B **96**, 144431 (2017). https://doi.org/10.1103/physrevb.96.144431
56. N. Biškup, J. Salafranca, V. Mehta, M.P. Oxley, Y. Suzuki, S.J. Pennycook, S.T. Pantelides, M. Varela, Insulating ferromagnetic $LaCoO_{3-\delta}$ films: a phase Induced by ordering of oxygen vacancies. Phys Rev Lett. **112**, 087202 (2014). https://doi.org/10.1103/physrevlett.112.087202
57. V.V. Mehta, N. Biskup, C. Jenkins, E. Arenholz, M. Varela, Y. Suzuki, Long-range ferromagnetic order in $LaCoO_{3-\delta}$ epitaxial films due to the interplay of epitaxial strain and oxygen vacancy ordering. Phys. Rev. B **91**, 144418 (2015). https://doi.org/10.1103/physrevb.91.144418
58. W.S. Choi, J.-H. Kwon, H. Jeen, J.E. Hamann-Borrero, A. Radi, S. Macke, R. Sutarto, F. He, G.A. Sawatzky, V. Hinkov, M. Kim, H.N. Lee, Strain-induced spin states in atomically ordered cobaltites. Nano Lett. **12**, 4966–4970 (2012). https://doi.org/10.1021/nl302562f
59. D. Shin, I. Kim, S. Song, Y. Seo, J. Hwang, S. Park, M. Choi, W.S. Choi, Defect engineering of magnetic ground state in $EuTiO_3$ epitaxial thin films. J. Am. Ceram. Soc. **104**, 4606–4613 (2021). https://doi.org/10.1111/jace.17870
60. W. Li, R. Zhao, L. Wang, R. Tang, Y. Zhu, J.H. Lee, H. Cao, T. Cai, H. Guo, C. Wang, L. Ling, L. Pi, K. Jin, Y. Zhang, H. Wang, Y. Wang, S. Ju, H. Yang, Oxygen-vacancy-induced antiferro magnetism to ferromagnetism transformation in $Eu_{0.5}Ba_{0.5}TiO_{3-\delta}$ multiferroic thin films. Sci Rep. **3**, 2618 (2013). https://doi.org/10.1038/srep02618
61. C. Menéndez, D. Chu, C. Cazorla, Oxygen-vacancy induced magnetic phase transitions in multiferroic thin films. Npj Comput. Mater. **6**, 76 (2020). https://doi.org/10.1038/s41524-020-0344-3
62. W. Niu, W. Liu, M. Gu, Y. Chen, X. Zhang, M. Zhang, Y. Chen, J. Wang, J. Du, F. Song, X. Pan, N. Pryds, X. Wang, P. Wang, Y. Xu, Y. Chen, R. Zhang, Direct demonstration of the emergent magnetism resulting from the multivalence Mn in a $LaMnO_3$ epitaxial thin film system. Adv. Electron. Mater. **4**, 1800055 (2018). https://doi.org/10.1002/aelm.201800055
63. A. Khan, S. Chatterjee, T.K. Nath, A. Taraphder, Defect-induced modulation of magnetic, electronic, and optical properties of the double-perovskite oxide La_2CoMnO_6. Phys. Rev. B **104**, 035152 (2021). https://doi.org/10.1103/physrevb.104.035152
64. G.D. Luca, J. Spring, M. Kaviani, S. Jöhr, M. Campanini, A. Zakharova, C. Guillemard, J. Herrero-Martin, R. Erni, C. Piamonteze, M.D. Rossell, U. Aschauer, M. Gibert, Top-layer engineering reshapes charge transfer at polar oxide interfaces. Adv. Mater. **34**, 2203071 (2022). https://doi.org/10.1002/adma.202203071
65. J.P. Palakkal, T. Schneider, L. Alff, Oxygen defect engineered magnetism of La_2NiMnO_6 thin films. AIP Adv. **12**, 035116 (2022). https://doi.org/10.1063/9.0000360